View metadata, citation and similar papers at core.ac.uk

brought to you by CORE

provided by CiteSeerX

Special Issue

New Insights Into Microaneurysms in the Deep Capillary Plexus Detected by Optical Coherence Tomography Angiography in Diabetic Macular Edema

Norio Hasegawa, Miho Nozaki, Noriaki Takase, Munenori Yoshida, and Yuichiro Ogura

Department of Ophthalmology and Visual Science, Nagoya City University Graduate School of Medical Sciences, Nagoya, Japan

Correspondence: Miho Nozaki, Department of Ophthalmology and Visual Science, Nagoya City University Graduate School of Medical Sciences, 1-Kawasumi, Mizuho-ku, Nagoya 467-8601, Japan; nozakim@med.nagoya-cu.ac.jp.

Submitted: December 2, 2015
Accepted: March 27, 2016

Citation: Hasegawa N, Nozaki M, Takase N, Yoshida M, Ogura Y. New insights into microaneurysms in the deep capillary plexus detected by optical coherence tomography angiography in diabetic macular edema. *Invest Ophthalmol Vis Sci*. 2016;57:OCT348–OCT355. DOI:10.1167/iovs.15-18782

Purpose. To study the association between the distributions of microaneurysms detected by en face optical coherence tomography angiography (OCTA) and diabetic macular edema (DME).

Methods. The study design was a retrospective chart review of 27 patients (33 eyes) with DME. The eyes were scanned using OCTA (6 × 6 mm) and spectral-domain (SD) OCT macular cube. Each of the images of the capillary plexus was overlaid onto the image of the topographic map, and the densities of the microaneurysms were measured by ImageJ software. The association between the distribution of microaneurysms and macular edema was evaluated.

Results. For microaneurysms in areas with and without edema, 77.3 ± 8.1% of these microaneurysms were located in the deep capillary plexuses (DCP). However, in areas of edema where the retinal thickness was more than 400 μm, 91.3 ± 9.1% of the microaneurysms were found in the DCP. This difference was statistically significant ($P < 0.001$). In the macular edema area, there was a significantly higher density of microaneurysms in the DCP compared to the superficial capillary plexuses (1.71/mm^2 vs. 0.17/mm^2, $P < 0.001$). There was also a significant correlation between the macular volume and the density of microaneurysms in the DCP in edema ($r = 0.63$, $P < 0.001$).

Conclusions. Our study demonstrated a high proportion of microaneurysms in the DCP, as well as a novel association between the distributions of microaneurysms detected by OCTA and DME. Results also indicated that microaneurysms located in the DCP contribute to the pathogenesis of DME.

Keywords: microaneurysms, diabetic macular edema, optical coherence tomography angiography

Diabetic macular edema (DME) is a leading cause of blindness in most industrialized nations.[1,2] Although the pathogenesis of DME remains unclear, it is thought to be related to the breakdown of the blood–retina barrier, leaking microaneurysms (MAs), and upregulated cytokine, among other factors. Enhanced expression of the proangiogenic cytokine vascular endothelial growth factor (VEGF)-A has been validated in patients with DME,[3,4] and anti-VEGF-A therapy is the current standard of care for DME.[5–7] However, this treatment requires repeated intravitreous injections for an indefinite period, and safety concerns regarding continual blockade of VEGF-A, which is constitutively expressed in the normal adult human retina, are emerging.[8–12] Although previous clinical studies for DME have proven that focal laser treatment for MAs is effective in focal edema that originated from leaking MAs,[13,14] other clinical studies that compared anti-VEGF therapy and focal laser treatment have shown the superiority of the anti-VEGF therapy in the treatment of DME.[5–7] Recently, precise focal photocoagulation using navigated laser photocoagulation combined with anti-VEGF antibody therapy showed promising efficacy for reducing the burden of the anti-VEGF agent.[15] To conduct precise focal photocoagulation, an accurate determination of the leaking MAs that are responsible for the edema is required. Currently, only fluorescein angiography can be used to clarify whether the type of edema is focal or diffuse and determine the leaking MAs. However, issues associated with the dye injection, such as renal dysfunction and anaphylaxis, are of concern for both patients and doctors.[16]

The use of optical coherence tomography (OCT) for in vivo vascular imaging was first reported for Doppler OCT, with this technique subsequently referred to as optical coherence angiography.[17] Recent developments have led to several new variations of the technique,[18–22] which are now collectively referred to as OCT angiography (OCTA). Optical coherence tomography angiography can be used to visualize the chorioretinal microcirculation without dye injection. The AngioVue system (Avanti OCT; Optovue, Fremont, CA, USA) using the split-spectrum amplitude decorrelation angiography (SSADA) algorithm can divide the retina–choroid layer into four layers: the superficial capillary plexuses (SCP), deep capillary plexuses (DCP), outer retina, and choroidal vessels.[23–28] Recent reports have demonstrated that OCTA can detect the characteristics of the vasculature in eyes with diabetic retinopathy.[29,30]

In the current study, we sought to further explore the association between the distribution and density of MAs detected by OCTA and macular edema detected by spectral-

This work is licensed under a Creative Commons Attribution-NonCommercial-NoDerivatives 4.0 International License.

Downloaded from iovs.arvojournals.org on 06/30/2019

domain (SD)-OCT (Cirrus HD-OCT; Carl Zeiss Meditec, Dublin, CA, USA) in patients with DME.

Methods

Patients

This study was a retrospective chart review of 33 eyes from 27 patients with DME who underwent en face OCT angiography and Cirrus HD-OCT at Nagoya City University Hospital between October 2014 and February 2015. This study was approved by the Institutional Review Board of the Nagoya City University Graduate School of Medical Science and was conducted in accordance with the ethical standards stated in the 1964 Declaration of Helsinki; it was registered at University hospital Medical Information Center (UMIN) (identification number: UMIN000015143). Eyes with OCT images of poor quality due to cataract or poor fixation, as well as eyes with epiretinal membrane or tractional retinal detachment, were excluded from the study. Eyes with OCT images that showed obvious segmentation error were also excluded.

Optical Coherence Tomography Angiography

Optical coherence tomography angiography images were obtained using RTVue XR Avanti OCT with AngioVue. AngioVue uses the SSADA algorithm to detect motion in the blood vessel lumen. This software makes it possible to noninvasively visualize the retinal and choroidal vasculature via motion contrast. Although OCTA can detect rapid blood flow in the vessels, it cannot visualize the leakage from capillaries or MAs. The AngioVue automatically segmented the retina–choroid layer into four layers that included the SCP, DCP, outer retina layer, and choriocapillaris. The SCP images include the vasculature from the inner limited membrane (ILM) to 15 μm under the inner plexiform layer (IPL), and encompass an area that contains vasculature projections from the retinal nerve fiber layer and ganglion cell layer. The DCP images include the vasculature from 15 μm under the IPL to 70 μm under the IPL, and encompass an area that contains the vascular plexuses at the border of the IPL and inner nuclear layer (INL) and the border of the INL and outer plexiform layer. The DCP images represent both the median and deep capillary plexus layers. All images collected in this study were 6×6 mm (Fig. 1A). Our current study utilized the automatic segmentation of the AngioVue software. Segmentation errors were found in several of the macular edema eyes in this study. When areas were lacking vasculature or included inappropriate vasculature, this was assumed to indicate the possibility of segmentation errors. Therefore, we carefully evaluated each of the OCTA images and the OCT B-scan images in detail, and then excluded from the study any eyes that exhibited obvious segmentation error (see Supplementary Fig. S1). Projection artifact was another problem associated with the OCTA. This artifact is caused by fluctuating shadows cast by flowing blood in the SCP that can cause variation of the OCT signal in deeper layers. Thus, the majority of the projection artifacts occurred in highly reflective layers such as the retinal pigment epithelium, while only a few projection artifacts were observed in the DCP.

Cirrus HD-OCT

When using RTVue XR Avanti OCT to detect the boundary of retinal edema, there is very little color contrast in the topographic map. Therefore, for these types of analyses, we used Cirrus HD-OCT imaging to capture the retinal topographic map (Fig. 2). Thus, this study used the topographic map of the macular cube images (6×6 mm) and the macular volume (MV) (mm^3) data for the analysis (Fig. 1B). Diabetic macular edema was classified into the following three types: serous retinal detachment (SRD), in which there was detachment of the sensory retina from the retinal pigment epithelium but no cystoid spaces at the presumed fovea; cystoid macular edema (CME), which presented predominantly as cystoid spaces within the area; and retinal swelling with no SRD or CME.[31,32]

Image Analysis

In each eye, we overlaid the retinal thickness topographic map obtained by the Cirrus HD-OCT onto the images of SCP and DCP obtained by OCTA using Adobe Photoshop (cs2; Adobe Systems, Inc., San Jose, CA, USA). Due to issues related to the color contrast of the topographic map, it was hard to identify the area where the retinal thickness was more than 300 or 350 μm (Fig. 2). Therefore, we defined the area where the retinal thickness was more than 400 μm (orange-red to white in the Cirrus HD-OCT color chart) as the area of edema. The measured area of the retinal edema (mm^2) and the number of MAs were determined by using the ImageJ software (developed by Wayne Rasband, National Institutes of Health, Bethesda, MD, USA; available in the public domain at http://rsb.info.nih.gov/ij/index.html).

The MAs in the SCP and DCP were measured separately. Based on the findings by Ishibazawa et al.,[29] we defined the MAs as round, saccular, or fusiform capillary dilation. We also separated the number of MAs inside of the retinal edema from the number of MAs outside of the retinal edema.

The number of MAs/mm^2 in the SCP and DCP was calculated as the density of the MAs. In addition, we also separately calculated the densities of the MAs inside and outside of the edema.

In order to emphasize the density of the MAs within the area of the edema, we calculated the ratio of the density of MAs (/mm^2) inside the edema to the density of the MAs (/mm^2) outside the edema.

We observed that some of the MAs that were located near the border were found in both the SCP and the DCP. Thus, we decided to select eight eyes at random and then evaluate the number of MAs that could be found at the same point in both the SCP and the DCP.

All measurements were performed twice by one inspector (NH) masked to the area of edema that was shown in the topographic map. Mean values of the two measurements were analyzed and used as the result. We also calculated the correlations for each of the values that were measured twice.

Statistics

All results are expressed as the mean ± SD. Data were collected and analyzed by a Student's *t*-test and the Tukey-Kramer test. For all statistical tests, $P < 0.05$ was considered as the significance level. Statistical analysis was performed using Ekuseru-Toukei 2012 (Social Survey Research Information Co., Ltd., Tokyo, Japan) and IBM SPSS Statistics for Windows, Version 22.0 (IBM Corp., Armonk, NY, USA). Pearson correlation coefficient was calculated to assess relationships between the number of MAs and the MV (mm^3), with $r^2 > 0.4$ considered to be strongly correlated.

Results

Patient Characteristics

Out of the 94 total eyes evaluated, 61 were excluded due to poor image quality caused by cataract and/or poor fixation and/or segmentation error. As a result, 33 eyes from 27 patients

Investigative Ophthalmology & Visual Science

Downloaded from iovs.arvojournals.org on 06/30/2019

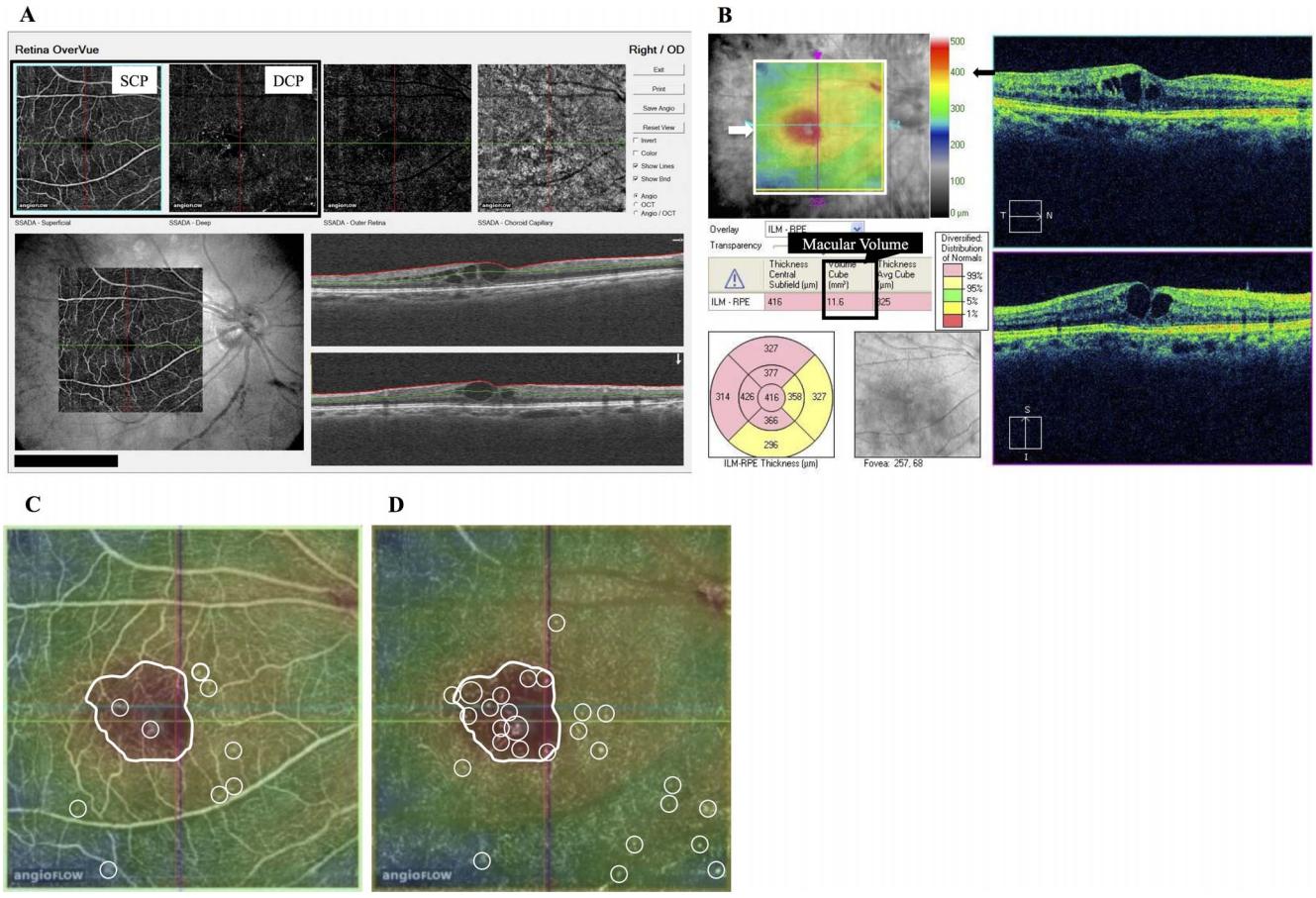

Figure 1. Representative images from the right eye of a 68-year-old female patient with CME-type DME. (**A**) Images obtained by RTVue XR Avanti OCT with AngioVue (6 × 6 mm); (**B**) Cirrus HD-OCT image; (**C**, **D**) overlaid images. (**A**) OCTA of the SCP, DCP, outer retina, and choriocapillaris are shown in the *upper row from left to right*, while the B-scan is shown in the *lower right*. (**B**) Retinal topographic map is depicted in the *left* image (*white arrow*), while the B-scans are seen on the *right*. The macular volume was automatically measured (11.6 mm^3). (**C**, **D**) Retinal topographic map of the HD-OCT was overlaid onto the OCTA of the SCP (**C**) and the DCP (**D**). Areas of the retina where the thickness was more than 400 µm are depicted *as orange-red to white* in the retinal topographic map (encircled by the *white line*, 1.971 mm^2). MAs are observed as round, saccular, or fusiform shapes of the dilated capillary (*white circles*).

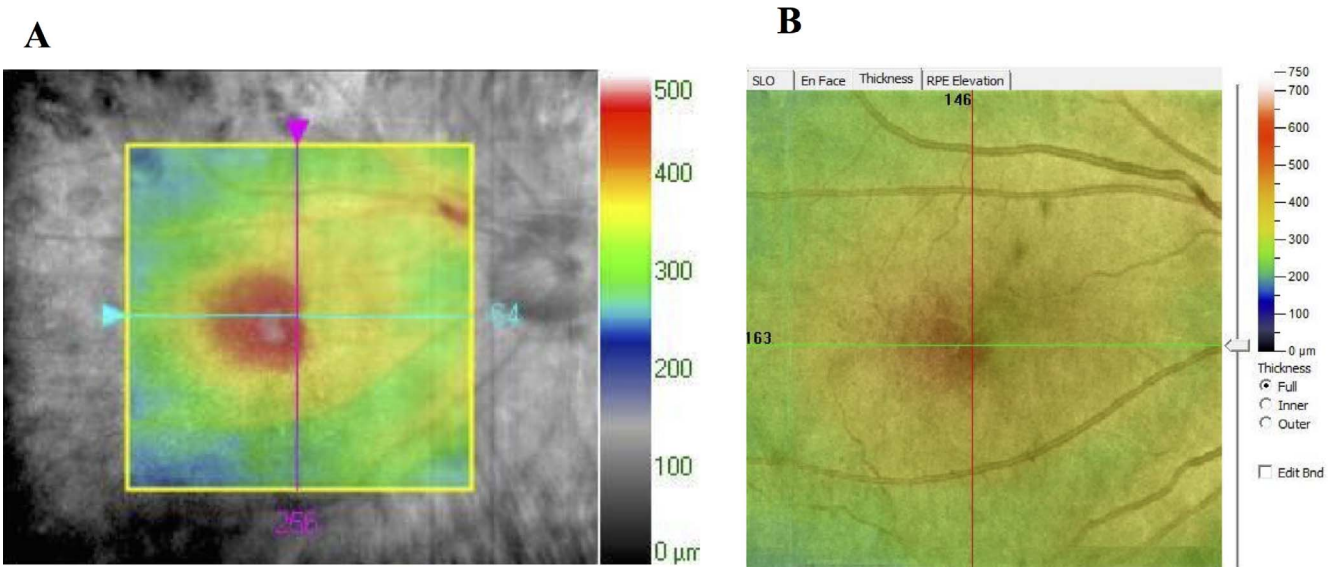

Figure 2. Topographic maps of the same eye taken by Cirrus HD-OCT (**A**) and RTVue XR Avanti OCT (**B**). The area of edema is defined by the strong contrast in the colors in the image obtained by the Cirrus HD-OCT. However, it was hard to identify areas where the retinal thickness was more than 300 or 350 µm even when using the topographic map obtained by the Cirrus HD-OCT. Therefore, the area of edema was defined as the area where the retinal thickness was more than 400 µm (*red to white* in the Cirrus HD-OCT color chart).

Investigative Ophthalmology & Visual Science

Downloaded from iovs.arvojournals.org on 06/30/2019

TABLE. Baseline Subject Characteristics

Characteristics	
No. of eyes (patients)	33 (27)
Mean age ± SD, y (range)	59.8 ± 10.8 (42–78)
Sex, male:female	16:11
Type of diabetes, type 1:type 2	0:27
Hemoglobin A1c (%), mean ± SD, available in 22 patients	7.4 ± 1.6
Mean BCVA, logMAR ± SD	0.21 ± 0.29
Diabetic retinopathy, nonproliferative:proliferative	19:14
Type of DME, CME type:retinal swelling type:SRD type	10:17:6
Macular volume, mm^3, mean ± SD	12.0 ± 1.4

SD, standard deviation; BCVA, best-corrected visual acuity.

(age, 42–78 years [59.8 ± 10.8 years]; sex, 16 males and 11 females) were included in the study for analysis. All had type 2 diabetes, with a mean value of glycated hemoglobin (HbA1c) of 7.4% (Table).

Patient classification included 14 eyes with proliferative diabetic retinopathy (PDR), 14 eyes with mild nonproliferative diabetic retinopathy (NPDR), and 5 eyes with moderate to severe NPDR. Of these, nine eyes had already undergone panretinal photocoagulation without macular laser, while four eyes had previously undergone pars plana vitrectomy.

The Density and Distribution of MAs in Each Capillary Plexus

Mean correlation coefficient between the two measurements was 0.93 (0.89–0.99) in counting MAs, and mean correlation coefficient was more than 0.99 in the edema measurement area (>400 μm).

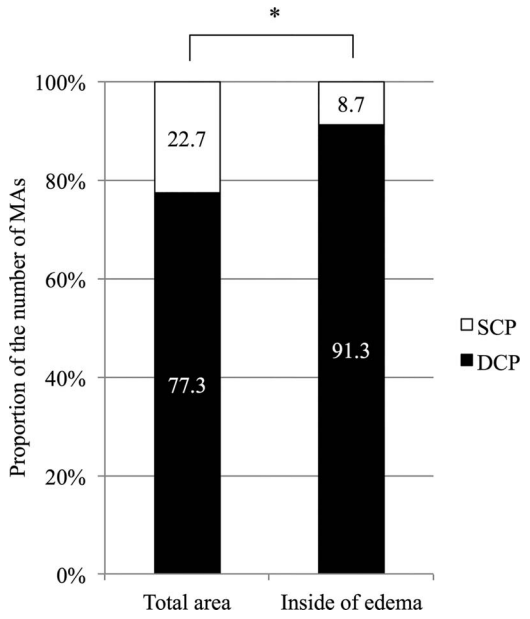

FIGURE 3. Graph shows the proportion of the number of MAs detected in the DCP and in the SCP for the total area (6 × 6 mm) and for inside of the edema area. In the DCP (total area), OCTA detected 77.3 ± 7.6% of the total MAs. Inside the area of edema, 91.3 ± 8.7% of the MAs were observed in the DCP. The difference in the proportion of the number of MAs between the total area and the area of edema was statistically significant (*$P < 0.001$).

For retinal edema, the mean area (>400 μm) for the 6 × 6–mm topographic map was 5.1 ± 4.5 mm^2 (0.5–22.1). The mean number of MAs detected by 6 × 6–mm en face OCT angiography was 17.2 ± 6.8 (6–29).

For the total number of MAs, 77.3 ± 7.6% of the MAs were located in the DCP, whereas in the retinal edema area, 91.3 ± 8.7% of the MAs were located in the DCP. There was a statistically significant difference between the two values ($P < 0.001$) (Fig. 3).

As seen in Figure 4, the analysis showed that there was no correlation between the ratio of the density of MAs in the DCP to the SCP and the total number of MAs ($r = 0.07$, $P = 0.69$).

The densities of the MAs (/mm^2) inside and outside of the edema in the SCP were 0.17 ± 0.25 and 0.10 ± 0.06, respectively. Likewise, the densities of the MAs (/mm^2) inside and outside of the edema in the DCP were 1.71 ± 1.21 and 0.24 ± 0.10, respectively (Fig. 5). Higher densities of MAs were found inside and outside of the edema in the DCP versus the SCP, with the highest density observed inside the edema in the DCP ($P < 0.001$).

In the eight eyes that were randomly selected from the subject group, 3.53 ± 1.55% (range, 0–7.40) of the total MAs were detected at the same point in both the SCP and the DCP.

The Correlation Between the Density of the MAs and the MV

Mean MV of the examined eyes was 11.88 ± 1.41 mm^3. Although there was a significant correlation between the density of MAs in the DCP and the MV ($r = 0.63$, $P < 0.001$) (Fig. 6A), there was a poor correlation between the density of MAs in the SCP and the MV ($r = 0.20$, $P = 0.27$) (Fig. 6B).

The Correlation Between the Density of the MAs and the Type of Macular Edema

To further investigate the association between the density of the MAs and the type of edema classified by SD-OCT, we evaluated the correlation between the ratio of the density of the MAs between inside and outside the edema in the DCP and the type of DME. Results showed there was a significantly higher ratio only for the CME type ($P < 0.05$) (Fig. 7).

DISCUSSION

Our current study examined the association between the distribution of MAs detected by OCTA and DME. Although the density of MAs in the SCP exhibited no significant difference between inside and outside of the edema, there was a significant increase in the density inside the edema in the DCP. These results demonstrated that the density of the MAs in the DCP was significantly associated with the MV. Moreover, our results also indicated that the MAs in the DCP contributed to the pathogenesis of DME, especially for the CME type of DME. To the best of our knowledge, this is the first study to evaluate the association between the distribution of MAs in each capillary plexus layer and DME using three-dimensional OCTA imaging.

Moore et al.[33] used immunohistochemistry to investigate human diabetic postmortem eyes, and showed that the majority of the MAs (approximately 80%) originated from the INL and therefore were in the deeper part of the inner retinal capillary plexus. Horii et al.[34] also reported that 80.3% of the MAs were located in the INL, while Ishibazawa et al.[29] used OCTA to examine diabetic eyes and showed that the MAs were mainly located in the deep plexus. Couturier et al.[30] used an OCTA 3 × 3–mm scan area and reported that the mean number

Investigative Ophthalmology & Visual Science

Downloaded from iovs.arvojournals.org on 06/30/2019

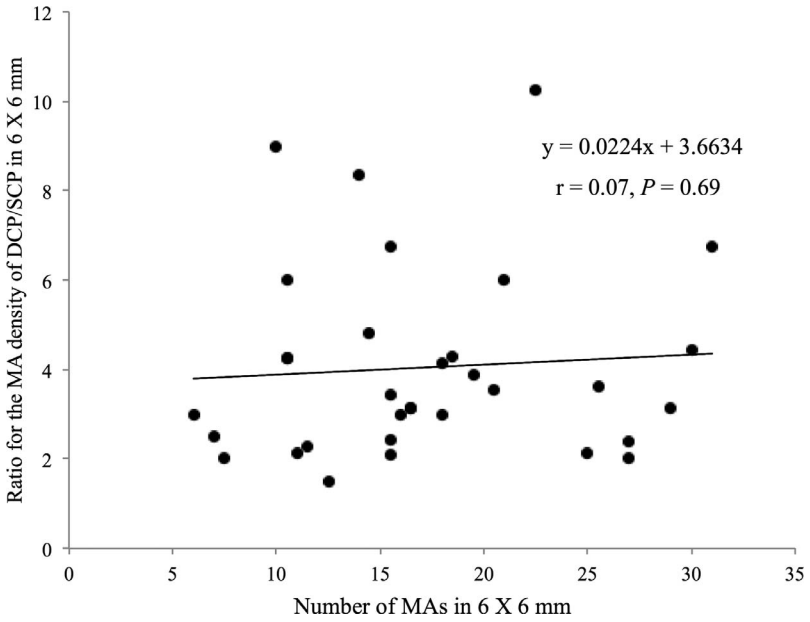

Figure 4. Scatter plot of the total number of MAs and ratio for the density of the MAs in the DCP to the SCP. There was no significant correlation observed ($r = 0.07$, $P = 0.69$).

of MAs located in the DCP was 4.4 while it was 2.9 in the SCP in the eyes with diabetic retinopathy. Although these previous studies did include diabetic eyes without DME, their findings were compatible with our current results, which showed that 77.3% of the MAs were located in the DCP.

Snodderly et al.[35] reported that the capillary network bracketing the INL, which contains the DCP, is more voluminous than the capillary network associated with the ganglion cell and nerve fiber layers, which contains the SCP. Anatomically, the majority of arteries and veins lie in the superficial vascular plexus, while the majority of capillaries lie in the deep plexus.[36] While the precapillary arterioles are enveloped by a single continuous layer of smooth muscle, the capillaries are surrounded only by pericytes.[37] Considering the distribution of the capillaries, we think it is reasonable that a majority of the MAs should be found in the DCP. In our study, we found no correlation between the ratio of the density of MAs in the DCP to the SCP and the total number of MAs. This indicates that the ratio of the number of MAs in the DCP to the SCP did not differ among the eyes examined, regardless of the severity of the diabetic retinopathy. These findings also support the hypothesis that the formation of MAs is primarily dependent on the vessel type, that is, capillaries or other vessels.

Previous OCT (B-scan) analysis has shown that MAs are the major source of focal fluid accumulation and are located deep

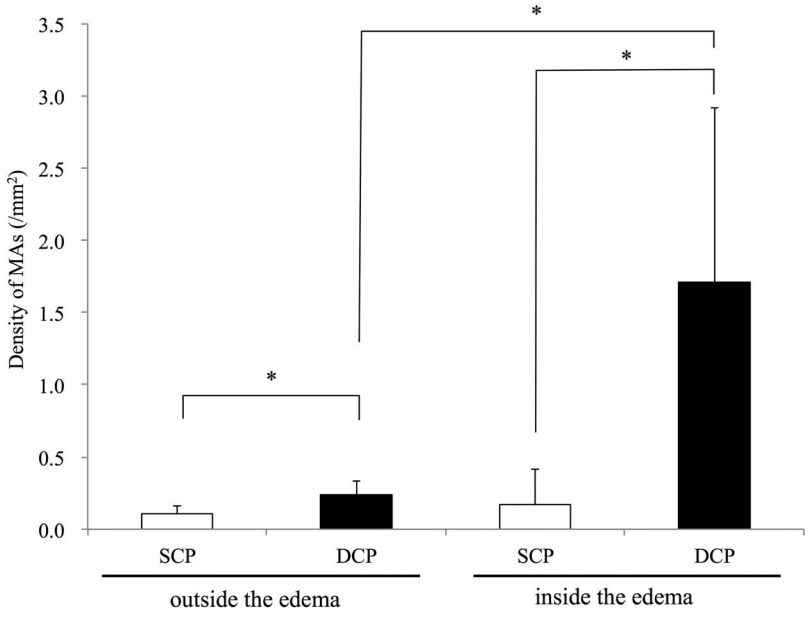

Figure 5. Densities (/mm²) of the MAs outside the edema in the SCP, MAs outside the edema in the DCP, MAs inside the edema in the SCP, and MAs inside the edema in the DCP were 0.10 ± 0.06, 0.24 ± 0.10, 0.17 ± 0.25, and 1.71 ± 1.21, respectively. Higher densities of MAs were found inside and outside the edema in the DCP versus the SCP, with the highest density observed inside the edema in the DCP (*$P < 0.001$).

Investigative Ophthalmology & Visual Science

Downloaded from iovs.arvojournals.org on 06/30/2019

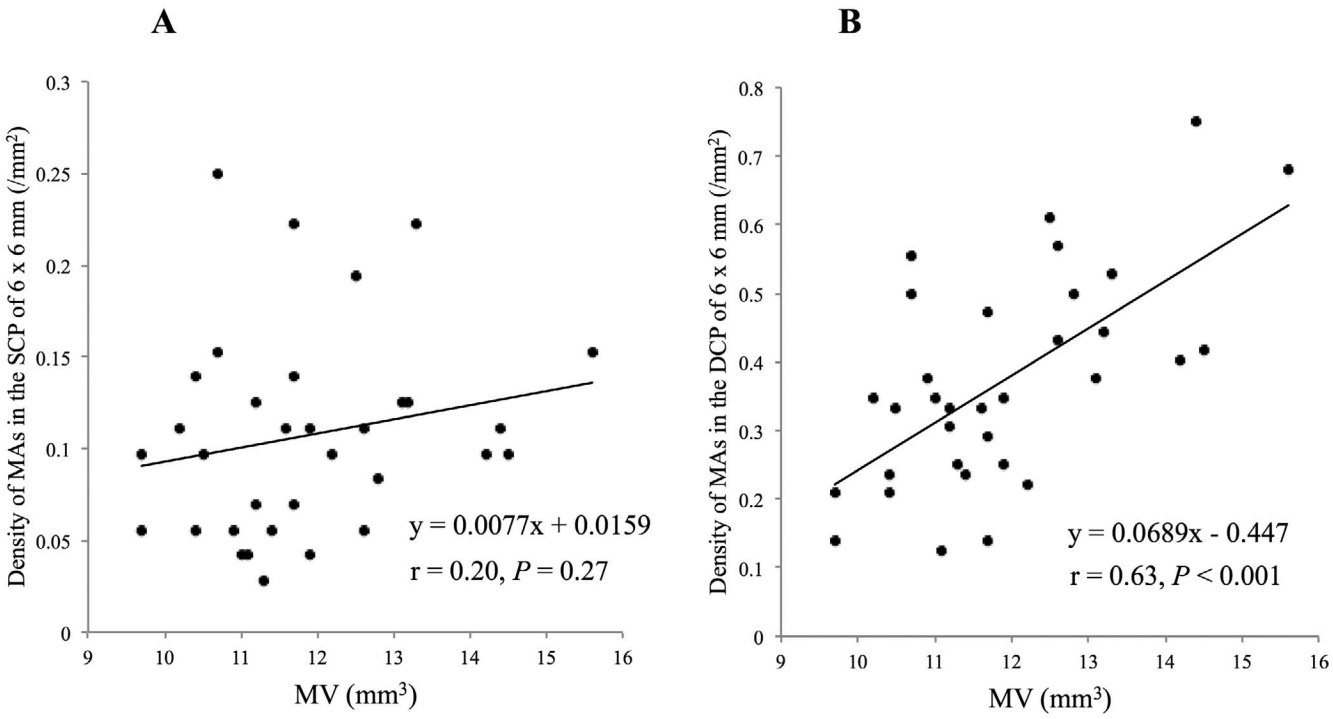

FIGURE 6. Scatter plots of the density of MAs in the SCP (**A**) and DCP (**B**) and the MV. A significant correlation was observed between the density of MAs in the DCP and the MV ($r = 0.63$, $P < 0.001$), whereas there was no correlation found between the density of MAs in the SCP and the MV ($r = 0.20$, $P = 0.27$).

inside the INL in focal edema.[38] Our current results also demonstrated that the MAs located in the DCP were significantly associated with the area of the edema, and that the density of the MAs in the DCP was significantly associated with the CME type of edema. Murakami et al.[32] reported that the CME type had significantly larger numbers of MAs compared with the SRD type or the retinal swelling type, and that the cystoid changes were usually located in the INL and outer plexiform layer.[33,35] These previous reports also support our speculation that the MAs in the DCP are responsible for pathogenesis of the CME type of edema.

Liegl et al.[15] reported that the use of precise focal laser photocoagulation for leaking MAs in conjunction with anti-VEGF therapy was a promising treatment option, as it reduced the number of additional anti-VEGF injections that were required. In order to detect leaking MAs, eyes need to be examined by fluorescein angiography. Unfortunately, some patients cannot tolerate the dye injection and thus fluorescein angiography cannot be used. In our present study, we used OCTA and demonstrated that there was a significant correlation between the MAs in the DCP and DME. Although OCTA cannot be used to visualize leakage, our results do indicate that OCTA might have use as a possible therapeutic approach for detecting MAs with adequate flow.

The limitations of our present study include the fact that it was a retrospective study and examined only a limited number of patients. In addition, in order to be able to quantify the distribution of the MAs, we excluded eyes with poor OCTA image quality. Although we evaluated 94 eyes, a total of 61 had to be excluded due to poor image quality caused by cataract and/or poor fixation and/or segmentation error. In addition, our exclusion criteria might have eliminated severe DME from the cases examined in this study. Furthermore, segmentation errors and projection artifacts have the potential to complicate OCTA analyses. In the current study, we found that there were several MAs that were located at the same point in both the

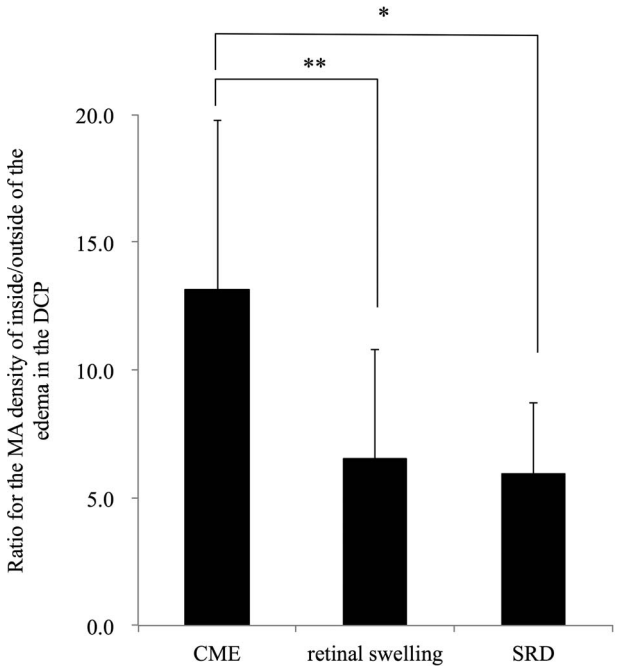

FIGURE 7. Graph shows that the ratios for MA density for the inside of the edema to the outside of the edema in the DCP were dependent on the three types of DME (CME type, retinal swelling type, and SRD type). Mean values were 13.2 ± 6.6, 6.5 ± 4.3, and 5.9 ± 2.8 in the CME type, retinal swelling type, and SRD type, respectively. The ratio was significantly higher in the CME type (*$P < 0.05$, **$P < 0.01$). There was no significant difference between the ratios for the retinal swelling type and the SRD type ($P = 0.969$).

Investigative Ophthalmology & Visual Science

Downloaded from iovs.arvojournals.org on 06/30/2019

SCP and the DCP. Thus, since these MAs were considered to be projection artifacts or to exist near the border of the segmentation, this could have led to errors during the counting of the MAs. To examine this potential problem, we subsequently tried to quantify the number of MAs that were found at the same point in the SCP and the DCP. Our results showed that less than 3.53% of all MAs were detected at the same point in the SCP and the DCP. This suggests that our results showing that the MAs in the DCP were associated with DME were not influenced by these errors. Also, our study did not compare MAs detected by OCTA with those detected by fluorescein angiography. Couturier et al.[30] reported that only 62% of MAs detected by fluorescein angiography could be visualized when using OCTA. Since OCTA can detect only blood flow, slow flow, or flow turbulence[29] in MAs, this might be the reason why visualization could not be achieved with use of OCTA. Since our findings did show that the MAs in the DCP were associated with DME, a further study that compares MAs detected by OCTA and by fluorescein angiography will need to be undertaken in the future.

In summary, the findings of our examination of the association between the distribution of MAs detected by OCTA and DME suggest that MAs in the DCP might contribute to the pathogenesis of DME. Optical coherence tomography angiography is a new technology that can divide the SCP and DCP, which makes it possible to perform a three-dimensional evaluation of the structure of edema. Our results additionally showed the potential benefit of being able to treat DME by targeting MAs detected by OCTA in the DCP.

Acknowledgments

The authors thank Fumie Shibuya, Yasuyo Matsuda, Ayano Maruyama, and Sayaka Oshio for their technical assistance.

Disclosure: **N. Hasegawa**, None; **M. Nozaki**, None; **N. Takase**, None; **M. Yoshida**, None; **Y. Ogura**, None

References

1. Moss SE, Klein R, Klein BE. Ten-year incidence of visual loss in a diabetic population. *Ophthalmology*. 1994;101:1061–1070.
2. Klein R, Klein BE, Moss SE, Cruickshanks KJ. The Wisconsin Epidemiologic Study of Diabetic Retinopathy: XVII. The 14-year incidence and progression of diabetic retinopathy and associated risk factors in type 1 diabetes. *Ophthalmology*. 1998;105:1801–1815.
3. Takagi H, Otani A, Kiryu J, Ogura Y. New surgical approach for removing massive foveal hard exudates in diabetic macular edema. *Ophthalmology*. 1999;106:249–257.
4. Funatsu H, Yamashita H, Noma H, et al. Increased levels of vascular endothelial growth factor and interleukin-6 in the aqueous humor of diabetics with macular edema. *Am J Ophthalmol*. 2002;133:70–77.
5. Mitchell P, Bandello F, Schmidt-Erfurth U, et al.; RESTORE study group. The RESTORE study: ranibizumab monotherapy or combined with laser versus laser monotherapy for diabetic macular edema. *Ophthalmology*. 2011;118:615–625.
6. Diabetic Retinopathy Clinical Research Network, Elman MJ, Qin H, et al. Intravitreal ranibizumab for diabetic macular edema with prompt versus deferred laser treatment: three-year randomized trial results. *Ophthalmology*. 2012;119:2312–2318.
7. Do DV, Nguyen QD, Boyer D, et al.; da Vinci Study Group. One-year outcomes of the da Vinci Study of VEGF Trap-Eye in eyes with diabetic macular edema. *Ophthalmology*. 2012;119:1658–1665.
8. Marneros AG, Fan J, Yokoyama Y, et al. Vascular endothelial growth factor expression in the retinal pigment epithelium is essential for choriocapillaris development and visual function. *Am J Pathol*. 2005;167:1451–1459.
9. Nishijima K, Ng YS, Zhong L, et al. Vascular endothelial growth factor-A is a survival factor for retinal neurons and a critical neuroprotectant during the adaptive response to ischemic injury. *Am J Pathol*. 2007;171:53–67.
10. Saint-Geniez M, Maharaj AS, Walshe TE, et al. Endogenous VEGF is required for visual function: evidence for a survival role on Muller cells and photoreceptors. *PLoS One*. 2008;3:e3554.
11. Saint-Geniez M, Kurihara T, Sekiyama E, et al. An essential role for RPE-derived soluble VEGF in the maintenance of the choriocapillaris. *Proc Natl Acad Sci U S A*. 2009;106:18751–18756.
12. Ueta T, Yanagi Y, Tamaki Y, Yamaguchi T. Cerebrovascular accidents in ranibizumab. *Ophthalmology*. 2009;116:362.
13. Photocoagulation for diabetic macular edema. Early Treatment Diabetic Retinopathy Study report number 1. Early Treatment Diabetic Retinopathy Study research group. *Arch Ophthalmol*. 1985;103:1796–1806.
14. Diabetic Retinopathy Clinical Research Network. A randomized trial comparing intravitreal triamcinolone acetonide and focal/grid photocoagulation for diabetic macular edema. *Ophthalmology*. 2008;115:1447–1449.
15. Liegl R, Langer J, Seidensticker F, et al. Comparative evaluation of combined navigated laser photocoagulation and intravitreal ranibizumab in the treatment of diabetic macular edema. *PLoS One*. 2014;9:e113981.
16. Bearelly S, Rao S, Fekrat S. Anaphylaxis following intravenous fluorescein angiography in a vitreoretinal clinic: report of 4 cases. *Can J Ophthalmol*. 2009;44:444–445.
17. Makita S, Hong Y, Yamanari M, et al. Optical coherence angiography. *Opt Express*. 2006;14:7821–7840.
18. Fingler J, Schwartz D, Yang C, et al. Mobility and transverse flow visualization using phase variance contrast with spectral domain optical coherence tomography. *Opt Express*. 2007;15:12636–12653.
19. Mariampillai A, Standish BA, Moriyama EH, et al. Speckle variance detection of microvasculature using swept-source optical coherence tomography. *Opt Lett*. 2008;33:1530–1532.
20. An L, Wang RK. In vivo volumetric imaging of vascular perfusion within human retina and choroids with optical micro-angiography. *Opt Express*. 2008;16:11438–11452.
21. Makita S, Jaillon F, Yamanari M, et al. Comprehensive in vivo micro-vascular imaging of the human eye by dual-beam-scan Doppler optical coherence angiography. *Opt Express*. 2011;19:1271–1283.
22. Kurokawa K, Sasaki K, Makita S, et al. Three-dimensional retinal and choroidal capillary imaging by power Doppler optical coherence angiography with adaptive optics. *Opt Express*. 2012;20:22796–22812.
23. Jia Y, Tan O, Tokayer J, et al. Split-spectrum amplitude-decorrelation angiography with optical coherence tomography. *Opt Express*. 2012;20:4710–4725.
24. Jia Y, Wei E, Wang X, et al. Optical coherence tomography angiography of optic disc perfusion in glaucoma. *Ophthalmology*. 2014;121:1322–1332.
25. Jia Y, Bailey ST, Wilson DJ, et al. Quantitative optical coherence tomography angiography of choroidal neovascularization in age-related macular degeneration. *Ophthalmology*. 2014;121:1435–1444.
26. Spaide RF, Klancnik JM Jr, Cooney MJ. Retinal vascular layers imaged by fluorescein angiography and optical coherence tomography angiography. *JAMA Ophthalmol*. 2015;133:45–50.
27. Savastano MC, Lumbroso B, Rispoli M. In vivo characterization of retinal vascularization morphology using optical coherence tomography angiography. *Retina*. 2015;35:2196–2203.

Investigative Ophthalmology & Visual Science

Downloaded from iovs.arvojournals.org on 06/30/2019

28. Bonnin S, Mané V, Couturier A, et al. New insight into the macular deep vascular plexus imaged by optical coherence tomography angiography. *Retina*. 2015;35:2347–2352.
29. Ishibazawa A, Nagaoka T, Takahashi A, et al. Optical coherence tomography angiography in diabetic retinopathy: a prospective pilot study. *Am J Ophthalmol*. 2015;160:35–44.
30. Couturier A, Mané V, Bonnin S, et al. Capillary plexus anomalies in diabetic retinopathy on optical coherence tomography angiography. *Retina*. 2015;35:2384–2391.
31. Otani T, Kishi S, Maruyama Y. Patterns of diabetic macular edema with optical coherence tomography. *Am J Ophthalmol*. 1999;127:688–693.
32. Murakami T, Nishijima K, Sakamoto A, et al. Foveal cystoid spaces are associated with enlarged foveal avascular zone and microaneurysms in diabetic macular edema. *Ophthalmology*. 2011;118:359–367.
33. Moore J, Bagley S, Ireland G, McLeod D, Boulton ME. Three dimensional analysis of microaneurysms in the human diabetic retina. *J Anat*. 1999;194:89–100.
34. Horii T, Murakami T, Nishijima K, et al. Optical coherence tomographic characteristics of microaneurysms in diabetic retinopathy. *Am J Ophthalmol*. 2010;150:840–848.
35. Snodderly DM, Weinhaus RS, Choi JC. Neural-vascular relationships in central retina of macaque monkeys (*Macaca fascicularis*). *J Neurosci*. 1992;12:1169–1193.
36. Lutty GA, Bhutto I, McLeod DS. Anatomy of the ocular vasculatures. In: Schmetterer L, Kiel JW, eds. *Ocular Blood Flow*. New York: Springer; 2012:16–20.
37. Archer DB, Gardiner TA, Stitt AW. Functional anatomy, fine structure and basic pathology of the retinal vasculature. In: Joussen AM, Gardner TW, Kirchhof B, Ryan SJ, eds. *Retinal Vascular Disease*. New York: Springer; 2007:3–6.
38. Byeon SH, Chu YK, Hong YT, et al. New insights into the pathoanatomy of diabetic macular edema: angiographic patterns and optical coherence tomography. *Retina*. 2012; 32:1087–1099.

Investigative Ophthalmology & Visual Science

Downloaded from iovs.arvojournals.org on 06/30/2019